

# La<sub>17</sub>Si<sub>9</sub>Al<sub>4</sub>N<sub>32-x</sub>O<sub>x</sub> ( $x \leq 1$ ): A Nitridoaluminosilicate with Isolated Si/Al-N/O Clusters

Guillaume Pilet,<sup>\*,[a],[b]</sup> Jekabs Grins,<sup>[a]</sup> Mattias Edén,<sup>[c]</sup> and Saeid Esmaeilzadeh<sup>[a]</sup>

**Keywords:** Aluminosilicates / Anions / Lanthanides

A nitrogen-rich aluminosilicate with nominal composition La<sub>17</sub>Si<sub>9</sub>Al<sub>4</sub>N<sub>33</sub> has been synthesised at 1500–1650 °C under a N<sub>2</sub> atmosphere by reaction of La metal, AlN and Si<sub>3</sub>N<sub>4</sub>. Its crystal structure was solved and refined in space group *F43m*, with  $a = 15.4279(6)$  Å and  $Z = 4$ , to  $R_f = 1.9\%$ . The structure contains two novel types of discrete tetrahedral aluminosilicate clusters, with respective nominal compositions Al<sub>4</sub>Si<sub>4</sub>N<sub>17</sub> and Si<sub>5</sub>N<sub>16</sub>, with La atoms in between. Bulk sam-

ples were also investigated by powder X-ray and electron diffraction. The <sup>29</sup>Si and <sup>27</sup>Al solid-state NMR results indicate that the phase contains minor amounts of oxygen and has a narrow compositional range with probable end limits La<sub>17</sub>Si<sub>9</sub>-Al<sub>4</sub>N<sub>33</sub> and La<sub>16.67</sub>Si<sub>9</sub>Al<sub>4</sub>N<sub>32</sub>O.

(© Wiley-VCH Verlag GmbH & Co. KGaA, 69451 Weinheim, Germany, 2006)

## Introduction

Nitridosilicates and sialons are well known to exhibit useful physical properties, such as high strength, good wear resistance, high decomposition temperature, good oxidation resistance, excellent thermal-shock properties and resistance to corrosive environments. They have traditionally been investigated with an aim towards applications such as cutting tools, burners, welding nozzles, heat exchangers and engine applications. Phase-formation conditions and phase-compatibility relationships have therefore been systematically studied in many M-Si-Al-O-N sialon systems [e.g. M = Ca, Y and rare-earth (RE) elements].<sup>[1]</sup> During the last decades, however, more efforts have also been directed towards the synthesis of novel compounds with more complex crystal structures.<sup>[2]</sup> In particular, the use of electropositive metals as starting materials has proven to be a successful synthesis route.<sup>[3]</sup> The new compounds found have crystal structures that exhibit features that are distinctly different from those found for oxosilicates.<sup>[4–6]</sup> For example, whereas the O atoms in oxosilicates are connected to either one or two Si atoms,<sup>[7]</sup> the N atoms in nitridosilicates and sialons may also be shared by three, and even four, Si tetrahedra.<sup>[8,9]</sup>

The network connectivity for nitridosilicates is therefore, as a rule, higher than for oxosilicates.

We report here on the structure determination and bulk synthesis of a new nitridoaluminosilicate with nominal composition La<sub>17</sub>Si<sub>9</sub>Al<sub>4</sub>N<sub>33</sub>. Two features make it noteworthy. First, its crystal structure does not contain any continuous linkage of tetrahedra, but instead two types of isolated Si-(Al)-N/(O) clusters. The same type of clusters is found in the similar structure of Pr<sub>63</sub>Si<sub>40</sub>Al<sub>12</sub>O<sub>20</sub>N<sub>115</sub>,<sup>[10]</sup> the first known example of a nitridosilicate structure with all Al and Si atoms in isolated clusters. However, Pr<sub>63</sub>Si<sub>40</sub>-Al<sub>12</sub>O<sub>20</sub>N<sub>115</sub> crystallises with a cubic *primitive* unit cell, in space group *P43m* with  $Z = 1$  and  $a = 15.185(2)$  Å, and the clusters are different with respect to their composition and connectivity, as described further below. Counterparts to the cluster types are also found in oxosilicate structures, although obviously they contain O instead of N atoms. Secondly, La<sub>17</sub>Si<sub>9</sub>Al<sub>4</sub>N<sub>33</sub> is, according to its formal composition, a rare example of a pure nitridoaluminosilicate. The few other members include the wurtzite-type phases MAl-SiN<sub>3</sub> (M = Be, Mg, Mn, Ca),<sup>[11,12]</sup> filled  $\alpha$ -Si<sub>3</sub>N<sub>4</sub>-type compounds,<sup>[13]</sup> Ca<sub>5</sub>Si<sub>2</sub>Al<sub>2</sub>N<sub>8</sub>,<sup>[12]</sup> and Ca<sub>4</sub>SiAl<sub>3</sub>N<sub>7</sub>.<sup>[12]</sup>

However, although it is clear that the phase is very rich in nitrogen, it cannot be ruled out that it may contain minor amounts of oxygen, considering, for example, that the starting materials were not free of oxygen. In order to obtain local structural insight, <sup>27</sup>Al and <sup>29</sup>Si NMR spectra were therefore recorded. The NMR results indicate that there is a minor substitution of N by O and that the phase is likely a solid solution with end limits La<sub>17</sub>Si<sub>9</sub>Al<sub>4</sub>N<sub>33</sub> and La<sub>16.67</sub>-Si<sub>9</sub>Al<sub>4</sub>N<sub>32</sub>O. In what follows, the nominal composition will first be assumed, the NMR results presented, and conclusions about compositional variations then addressed in the Discussion.

[a] Arrhenius Laboratory, Division of Inorganic Chemistry, Stockholm University, 10691 Stockholm, Sweden

[b] Laboratoire des Multimatériaux et Interfaces, Groupe de Cristallographie et Ingénierie Moléculaire, Université Claude Bernard Lyon 1, Bâtiment Jules Raulin, Campus de la Doua, 69622 Villeurbanne Cedex, France  
E-mail: guillaume.pilet@univ-lyon1.fr

[c] Arrhenius Laboratory, Division of Physical Chemistry, Stockholm University, 106 91 Stockholm, Sweden

## Results

## Crystal Structure Determination and Refinement

The single-crystal data for  $\text{La}_{17}\text{Si}_9\text{Al}_4\text{N}_{33}$  could be indexed with a cubic F-centred unit cell with  $a = 15.410(1)$  Å. The F-centring, and the absence of further reflection conditions, was confirmed by electron diffraction (ED). The [011] zone axis pattern in Figure 1a shows the absence of  $00l$  reflections with  $l \neq 2n$  and  $hk0$  reflections with  $h + k \neq 2n$ . Tilting of the sample (see Figure 1b) showed that an equivalent set of reflections appear in the first-order Laue zone (FOLZ), thus implying the extinction symbol  $F\bar{4}3m$ .<sup>[14]</sup> The structure was solved in the space group  $F\bar{4}3m$  by direct methods, using the SIR97 program<sup>[15]</sup> in combination with Fourier difference syntheses. It was refined against  $F$  using the CRYSTALS program<sup>[16]</sup> and reflections with  $I/\sigma(I) > 3$ . An inspection of refined atomic positions showed that the space group symmetry could be increased to  $F\bar{4}3m$  (no. 216), and the final refinements made using this space group yielded a weighted  $R_f$  value of 1.9% for 294 unique reflections.

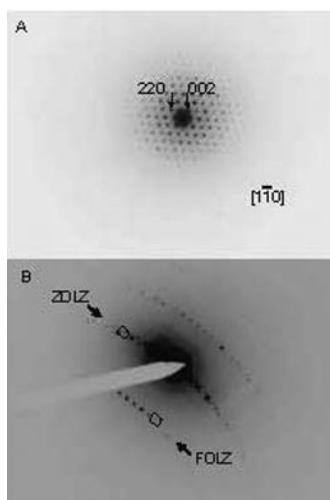


Figure 1.(a) [011] zone axis ED pattern of  $\text{La}_{17}\text{Si}_9\text{Al}_4\text{N}_{33}$ , showing the absence of  $00l$  reflections with  $l \neq 2n$  and  $hk0$  reflections with  $h + k \neq 2n$ . (b) A corresponding tilted ED pattern, showing an equivalent set of reflections in the first-order Laue zone (FOLZ).

Table 1. Atomic parameters for  $\text{La}_{17}\text{Si}_9\text{Al}_4\text{N}_{33}$ ; cubic,  $a = 15.4279(6)$  Å,  $V = 3672.13$  Å<sup>3</sup>,  $F\bar{4}3m$ ,  $Z = 4$ .

| Atom | Site | $x$        | $y$        | $z$         | $U_{\text{eq}}$ [Å <sup>2</sup> ] |
|------|------|------------|------------|-------------|-----------------------------------|
| La1  | 24f  | 1/2        | 0.29365(6) | 0           | 0.0098                            |
| La2  | 24g  | 3/4        | 1/4        | 0.01012(8)  | 0.0141                            |
| La3  | 16e  | 0.40995(6) | 0.09005(6) | -0.09005(6) | 0.0230                            |
| La4  | 4d   | 3/4        | 1/4        | 1/4         | 0.0176                            |
| Si1  | 4a   | 1/2        | 1/2        | 0           | 0.0064                            |
| Si2  | 16e  | 0.6354(3)  | 0.1354(3)  | -0.1354(3)  | 0.0107                            |
| Si3  | 16e  | 0.6338(3)  | 0.3662(3)  | 0.1338(3)   | 0.0070                            |
| Al1  | 16e  | 0.8199(3)  | 0.1801(3)  | -0.1801(3)  | 0.0116                            |
| N1   | 48h  | 0.6134(5)  | 0.2577(7)  | 0.1134(5)   | 0.013(3)                          |
| N2   | 48h  | 0.3854(6)  | 0.2476(8)  | 0.1146(6)   | 0.029(3)                          |
| N3   | 16e  | 0.5665(8)  | 0.4335(8)  | 0.0665(8)   | 0.013(4)                          |
| N4   | 16e  | 0.575(1)   | 0.075(1)   | -0.075(1)   | 0.054(8)                          |
| N5   | 4c   | 3/4        | 1/4        | -1/4        | 0.02(1)                           |

tions. Thermal displacement parameters were refined anisotropically for Si and La atoms, and isotropically for N atoms. Refinement data are given in the Experimental Section, with structural parameters in Table 1 and selected bond lengths in Table 2.

Table 2. Atomic distances [Å] in  $\text{La}_{17}\text{Si}_9\text{Al}_4\text{N}_{33}$ .

| Si–N   |             |        |             | Average |              |
|--------|-------------|--------|-------------|---------|--------------|
| Si1–N3 | 1.77(2) 4×  |        |             | 1.77    |              |
| Si2–N2 | 1.79(1) 3×  | Si2–N4 | 1.63(3)     | 1.75    |              |
| Si3–N1 | 1.73(1) 3×  | Si3–N3 | 1.80(2)     | 1.75    |              |
| Al–N   |             |        |             |         |              |
| Al1–N2 | 1.81(1) 3×  | Al1–N5 | 1.866(7)    | 1.82    |              |
| La–N   |             |        |             |         |              |
| La1–N1 | 2.53(1) 2×  | La1–N2 | 2.60(1) 2×  | La1–N3  | 2.5971(9) 2× |
| La2–N1 | 2.642(2) 4× | La2–N2 | 2.837(1) 4× |         |              |
| La3–N4 | 2.56(2) 3×  | La3–N1 | 2.63(1) 3×  |         |              |
| La4–N1 | 2.98(1) 12× |        |             |         |              |

## Structure Description

The unit cell contains four nominal formula units of  $\text{La}_{17}\text{Si}_9\text{Al}_4\text{N}_{33}$ . Possible deviations from this formula are addressed in the Discussion. There are four tetrahedral T (T = Si/Al) sites in the structure. One site has a considerably larger average T–N distance than the other ones and is concluded to be occupied by Al atoms. The other three T sites are accordingly occupied by only Si atoms. The structure contains two types of isolated tetrahedral clusters. One type has a composition of  $\text{Al}_4\text{Si}_4\text{N}_{17}^{-23}$  and is illustrated in Figure 2 (a). In each  $\text{Al}_4\text{Si}_4\text{N}_{17}$  unit, a central N atom, on the

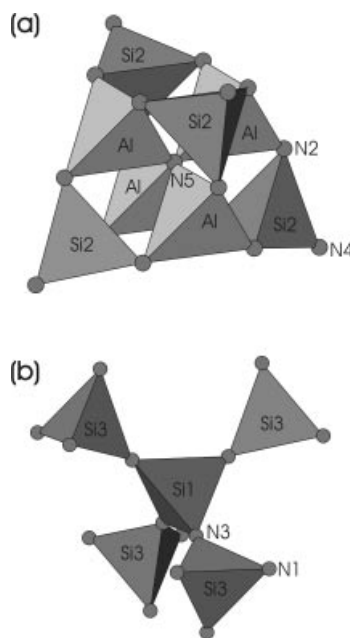


Figure 2. The two types of tetrahedral clusters found in the structure of  $\text{La}_{17}\text{Si}_9\text{Al}_4\text{N}_{33}$ . (a) The  $\text{Al}_4\text{Si}_4\text{N}_{17}$  cluster centred at the  $4c$  site at  $(1/4, 1/4, 1/4)$ . (b) The  $\text{Si}_5\text{N}_{16}$  cluster centred at the  $4a$  site at  $(0, 0, 0)$ .

4c site at (1/4,1/4,1/4), is common to four  $\text{AlN}_4$  tetrahedra. Each of four  $\text{SiN}_4$  tetrahedra then shares three of its N corner atoms with separate  $\text{AlN}_4$  tetrahedra, and has one free apex N atom pointing outwards from the unit. A crystal-chemical formula<sup>[17]</sup> for the crystal is  $[\text{Al}_4^{1:6}\text{Si}(2)_4^{1:3}\text{N}(4)^{1:1}\text{N}(2)_{12}^{2:2}\text{N}(5)^{4:4}]^{23-}$ . A similar cluster is found in the structure of  $\text{Pr}_{63}\text{Si}_{40}\text{Al}_{12}\text{O}_{20}\text{N}_{115}$ .<sup>[10]</sup> This has the composition  $\text{Al}_4\text{Si}_4\text{N}_{13}\text{O}_4^{-19}$  and differs by having O atoms on the Si tetrahedra apex atom sites. An identical atomic arrangement is also found for the  $\text{Be}_4\text{Si}_4\text{O}_{17}$  cluster in the structure of  $\text{Na}_{10}\text{Be}_4\text{Si}_4\text{O}_{17}$ .<sup>[18]</sup>

The other type of cluster, illustrated in Figure 2 (b), has a composition of  $\text{Si}_5\text{N}_{16}^{-28}$  and a crystal-chemical formula of  $[\text{Si}(1)^{1:4}\text{Si}(3)_3^{1:1}\text{N}(1)_{12}^{1:1}\text{N}(3)^{2:2}]^{28-}$ . It has at its centre, on the 4a site at (0,0,0), a  $\text{SiN}_4$  tetrahedron that is connected by corner-sharing to four surrounding  $\text{SiN}_4$  tetrahedra. Similar clusters, with composition  $\text{Si}_5\text{N}_{16}$ , are found in the structure of zunyite  $[\text{Al}_{13}\text{Si}_5\text{O}_{20}(\text{OH})_{18}\text{Cl}]$ .<sup>[19]</sup> The structure of  $\text{Pr}_{63}\text{Si}_{40}\text{Al}_{12}\text{O}_{20}\text{N}_{115}$  also contains  $\text{Si}_5\text{N}_{16}$  zunyite-type clusters, but four such clusters are further interlinked by four additional  $\text{SiON}_3$  tetrahedra to form a much larger cluster with composition  $\text{Si}_{24}\text{N}_{64}\text{O}_4^{-104}$ . The arrangement of two types of clusters in the unit cell of  $\text{La}_{17}\text{Si}_9\text{Al}_4\text{N}_{33}$

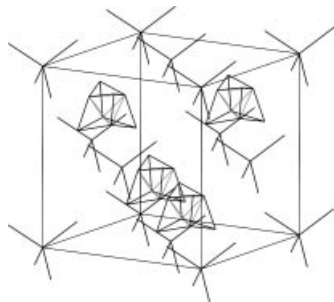


Figure 3. An illustration of the arrangement of the two types of clusters in the unit cell of  $\text{La}_{17}\text{Si}_9\text{Al}_4\text{N}_{33}$ . The drawn lines connect tetrahedral atom positions.

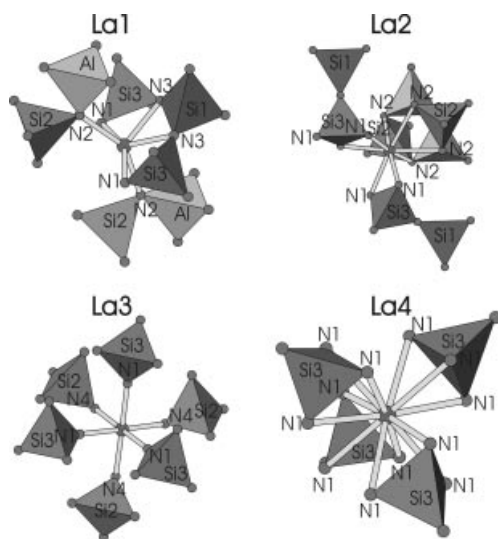


Figure 4. The coordination of N atoms around the four crystallographically different La atoms in the structure of  $\text{La}_{17}\text{Si}_9\text{Al}_4\text{N}_{33}$ .

is illustrated in Figure 3. There are four different La atom positions in the structure; the coordination of N atoms around them is illustrated in Figure 4. La1 is coordinated by six N atoms at 2.53–2.60 Å that form a distorted square bipyramid, La2 by a distorted cube of eight N atoms at 2.64–2.84 Å, La3 by a distorted octahedron of six N atoms at 2.56–2.63 Å, and La4 by 12 N atoms that form a cube-octahedron.

### Bulk Synthesis

Initial syntheses showed that the  $\text{La}_{17}\text{Si}_9\text{Al}_4\text{N}_{33}$  phase could be obtained together with LaN in the presence of a large excess (double amount) of La metal. The crystallinity was good, but the sample decomposed over a period of about one week, simultaneously with hydrolysis of the LaN, when left in contact with air. When stoichiometric amounts of the starting materials were used, and also when adding a smaller excess (10%) of La, yellow to yellow-green coloured samples were obtained after applying two consecutive heat treatments at 1500 and 1600 °C. These samples contained two minority phases in addition to  $\text{La}_{17}\text{Si}_9\text{Al}_4\text{N}_{33}$ . The reflections of one could be indexed using a small monoclinic unit cell with  $a = 5.2582(9)$ ,  $b = 5.5717(9)$ ,  $c = 3.9909(6)$  Å, and  $\beta = 92.35(1)^\circ$ , thus indicating that its structure may be perovskite related. The reflections of the second could be indexed with an *I*-centred tetragonal unit cell with  $a = 6.821(2)$  and  $c = 11.133(6)$  Å. The cell strongly suggests that the phase is related to  $\text{La}_3\text{AlO}_3\text{N}_2$ , which crystallises in *I4/mcm* with  $a = 6.855(2)$  and  $c = 11.199(5)$  Å.<sup>[20]</sup> A third heat treatment did not decrease the amounts of these secondary phases. However, their amounts could be drastically reduced by mixing the obtained samples with 3 wt.-% fine-grained carbon and then further heat-treating them at 1500 °C, i.e. by a carbothermal reduction and nitridation of the secondary phases. The powder pattern of the stoichiometric, yellow sample then only contained two weak reflections, with relative intensities below 1.5%, for the impurity phases. A good agreement was found between the observed reflection intensities and the intensities calculated from the single crystal data. The obtained unit-cell parameter was  $a = 15.4279(6)$  Å and the indexed powder pattern is given in Table 3. Unfortunately, we were not able to obtain samples with this level of purity in larger amounts, for example to perform neutron powder diffraction or physical property measurements.

To find an alternative synthetic route, a 4-g stoichiometric mixture of LaN,  $\text{Si}_3\text{N}_4$  and AlN was hot-pressed at 1600 °C and 50 MPa for 4 h. The powder pattern of the prepared sample contained, however, only broad reflections from unreacted starting materials, cuspidine-type  $\text{La}_4\text{Si}_2\text{O}_7\text{N}_2$  and unidentified phases. In order to investigate whether Al and O can be simultaneously incorporated into  $\text{La}_{17}\text{Si}_9\text{Al}_4\text{N}_{33}$  according to the common sialon substitution mechanism ( $\text{Si}^{4+} + \text{N}^{3-} \leftrightarrow \text{Al}^{3+} + \text{O}^{2-}$ ) three 1.5-g samples of  $\text{La}_{17}\text{Si}_{9-x}\text{Al}_{4+x}\text{N}_{33-x}\text{O}_x$ , with  $x = 2, 4$ , and 6, were prepared with  $\text{SiO}_2$  as oxygen source. The powder patterns of

Table 3. Observed and calculated  $2\theta$  values for the Guinier–Hägg diffraction pattern of  $\text{La}_{17}\text{Si}_9\text{Al}_4\text{N}_{33}$  up to the 20th observed line.  $a = 15.4279(6)$  Å,  $\Delta 2\theta = 2\theta_{\text{obs.}} - 2\theta_{\text{calcd.}}$ ,  $\lambda = 1.5406$  Å. Cell figure-of-merit:  $M_{20} = 131$ ,  $F_{20} = 152$  (0.0055, 24).

| <i>hkl</i> | $2\theta_{\text{obs.}}$ [°] | $\Delta 2\theta$ | $d_{\text{obs}}$ [Å] | $I/I_0$ |
|------------|-----------------------------|------------------|----------------------|---------|
| 111        | 9.930                       | 0.007            | 8.90                 | 12      |
| 220        | 16.233                      | −0.004           | 5.45                 | 1       |
| 400        | 23.046                      | 0.005            | 3.856                | 36      |
| 331        | 25.139                      | −0.001           | 3.540                | 20      |
| 420        | 25.813                      | 0.008            | 3.449                | 6       |
| 422        | 28.320                      | 0.003            | 3.149                | 28      |
| 511        | 30.067                      | −0.007           | 2.970                | 83      |
| 440        | 32.805                      | −0.007           | 2.728                | 100     |
| 600        | 34.871                      | 0.007            | 2.571                | 13      |
| 620        | 36.814                      | −0.002           | 2.440                | 1       |
| 533        | 38.218                      | −0.005           | 2.353                | 3       |
| 622        | 38.697                      | 0.015            | 2.325                | 5       |
| 444        | 40.473                      | −0.002           | 2.227                | 21      |
| 711        | 41.774                      | −0.005           | 2.161                | 5       |
| 640        | 42.199                      | −0.007           | 2.140                | 2       |
| 642        | 43.879                      | −0.001           | 2.062                | 5       |
| 731        | 45.100                      | −0.003           | 2.009                | 12      |
| 800        | 47.081                      | −0.005           | 1.929                | 10      |
| 733        | 48.242                      | −0.003           | 1.885                | 10      |
| 820        | 48.640                      | 0.013            | 1.870                | 7       |

the samples with  $x = 2$  and 4 showed no change in the unit-cell parameter for  $\text{La}_{17}\text{Si}_9\text{Al}_4\text{N}_{33}$  and the presence of several additional phases, among them AlN and the two secondary phases described above. The sample with  $x = 6$  contained no  $\text{La}_{17}\text{Si}_9\text{Al}_4\text{N}_{33}$  at all. These results show that the  $\text{La}_{17}\text{Si}_9\text{Al}_4\text{N}_{33}$  phase does not accept any significant simultaneous incorporation of Al and O. A comparison of the obtained unit-cell parameters for all preparations of  $\text{La}_{17}\text{Si}_9\text{Al}_4\text{N}_{33}$  showed, however, very small but significant variations. The largest unit-cell parameter was observed for the sample prepared with a large excess of La [ $a = 15.4402(9)$  Å], and the smallest one for the stoichiometric sample that was further heat-treated with added carbon at 1500 °C [ $a = 15.4279(6)$  Å]. The difference is very small [0.012(1) Å], but indicates nevertheless that  $\text{La}_{17}\text{Si}_9\text{Al}_4\text{N}_{33}$  shows smaller compositional variations. It may be noted that the two samples have nominally the same Al/Si ratio. Finally, attempts were made to prepare isostructural phases with the rare-earths Pr, Sm, Gd and Y at 1500–1650 °C. These were not successful, but in the case of Y yielded a very distinct powder pattern from YN and a hexagonal phase with  $a = 9.8027(4)$  and  $c = 10.6235(6)$  Å. The unit-cell parameters indicate that the phase is isostructural with  $\text{Y}_{6+x/3}\text{Si}_{11}\text{N}_{20+x}\text{O}_{1-x}$ ,<sup>[21]</sup> a structure type that can also incorporate Al according to the more general formula  $\text{RE}_{6+x/3}\text{Si}_{11-y}\text{Al}_y\text{N}_{20+x+y}\text{O}_{1-x+y}$ , e.g.  $\text{Nd}_7\text{Si}_8\text{Al}_3\text{N}_{20}$ .<sup>[22]</sup>

## Solid-State NMR Spectroscopy

### <sup>27</sup>Al NMR

Figure 5 shows <sup>27</sup>Al MAS and 3QMAS<sup>[24]</sup> NMR spectra recorded for a freshly prepared sample of  $\text{La}_{17}\text{Si}_9\text{Al}_4\text{N}_{33}$ . The MAS spectrum displays two signals at around  $\delta = 112$

and 90 ppm, which were assigned to  $\text{AlN}_4$  and  $\text{AlN}_3\text{O}$  tetrahedra, respectively, on the basis of typical chemical shifts for such units.<sup>[25,26]</sup>

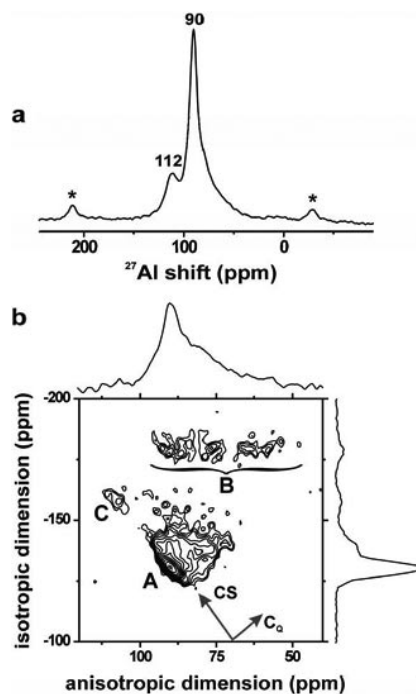


Figure 5. (a) Zoom around the centre-band region of an <sup>27</sup>Al MAS spectrum recorded for  $\text{La}_{17}\text{Si}_9\text{Al}_4\text{N}_{33}$  at a MAS frequency of 12.5 kHz. It results from the summation of 192 signal transients, each obtained using a relaxation delay of 200 s and short excitation pulse of flip angle ca. 12°. The nutation frequency was 94 kHz, measured relative to  $\text{Al}^{3+}(\text{aq})$ . 200 Hz full width at half maximum height (FWHM) Lorentzian broadening was applied prior to Fourier transformation. Chemical shift values are displayed on the top of the peak maxima and asterisks indicate spinning sidebands. (b) 3QMAS spectrum recorded by the shifted-echo technique<sup>[23]</sup> at 13.3 kHz MAS, using 96 transients per  $t_1$ -value and relaxation delays of 30.5 s. Arrows indicate the direction of peak displacement due to changes in isotropic chemical shifts and quadrupolar coupling constants.

However, the higher spectral resolution in the 3QMAS spectrum reveals a significantly more complex signal pattern than hinted from the 1D MAS spectrum. The signal region labelled A corresponds to the peak at  $\delta = 90$  ppm in the MAS spectrum. From the 3QMAS data, we estimated the isotropic chemical shift as  $\delta_{\text{iso}} = 92$  ppm. As the asymmetry parameter of the electric-field tensor could not be determined for any of the sites discussed below, we have henceforth assumed that  $\eta = 0$ , for site A, which results in a corresponding quadrupolar coupling constant  $C_Q = e^2qQ/h = 1.7$  MHz. The same chemical shift value was obtained by using the frequency positions of central and satellite transition peaks, as described previously.<sup>[26]</sup> Signal A extends along both spectral dimensions due to spreads in isotropic chemical shifts as well as quadrupolar coupling constants. In the MAS spectrum in part a of Figure 5, these dispersions are manifested as the signal “tail” extending towards lower shifts (ppm values). However, the broad peak labelled B (Figure 5, b) also contributes to this spectral re-



gion. Signal B is associated with an aluminium site experiencing a significant quadrupolar coupling constant (estimated as  $CQ = 7.4$  MHz), but unlike the other sites, it is not associated with dispersions in quadrupolar couplings or chemical shifts. Based on its isotropic chemical shift ( $\delta_{\text{iso}} = 108$  ppm), this peak is assigned to an  $\text{AlN}_4$  environment.<sup>[25,26]</sup>

The 3QMAS spectral intensities are not quantitative<sup>[24]</sup> due to the widely differing quadrupolar coupling constant of site B compared to A and C. This is evident, for example, from the fact that the anisotropic MAS projection of Figure 5 (b) differs from the 1D MAS spectrum in Figure 5 (a), as is the incomplete excitation of the peak around  $\delta = 112$  ppm (corresponding to signal C in Figure 5, b).

The MAS spectrum was deconvoluted into three components (not shown), from which the relative integrated intensities for A–C were estimated. This (highly uncertain) calculation showed that 55, 34 and 11% of the total signal portion derives from A, B and C, respectively. It now remains to reconcile the information from the  $^{27}\text{Al}$  NMR spectrum, which shows signals from (at least) three distinct Al environments (for the proposed structure of  $\text{La}_{17}\text{Si}_9\text{Al}_4\text{N}_{33}$  only a *single* tetrahedral  $\text{AlN}_4$  site is expected). Several scenarios of  $\text{O} \leftrightarrow \text{N}$  and  $\text{Si} \leftrightarrow \text{Al}$  substitution were considered. It turned out to be most plausible that (i) the weak signal C derives from a minor impurity phase that is not detected by XRD (incidentally, its NMR parameters are almost identical to those of  $\text{AlN}$ ) and (ii) the remaining two sites may be accounted for by noting that if oxygen substitutes for nitrogen at the  $4c$  position, four  $\text{AlN}_4$  units are converted into four  $\text{AlN}_3\text{O}$  units for every  $\text{N} \rightarrow \text{O}$  replacement. After renormalising the integrals of A and B, this implies that the structure contains 62%  $\text{AlN}_3\text{O}$  and 38%  $\text{AlN}_4$  units, which translates roughly into 62% oxygen substitution at the  $4c$  positions and the net formula  $\text{La}_{17}\text{Si}_9\text{Al}_4\text{N}_{32.4}\text{O}_{0.6}$ .

### $^{29}\text{Si}$ NMR

The corresponding  $^{29}\text{Si}$  MAS spectrum is shown in Figure 6. It has a poor signal-to-noise ratio due to the very slow  $^{29}\text{Si}$   $T_1$  relaxation coupled to relatively broad NMR signals, and displays two main groups of peaks, one extending between  $\delta = -51$  and  $-56$  ppm and another centred at  $\delta = -70$  ppm. Both signals are attributed to  $\text{SiN}_4$  tetrahedra. However, whereas the chemical shift of the former peak is representative for such units, a shift of around  $\delta = -70$  ppm is more typical of  $\text{SiN}_2\text{O}_2$  groups.<sup>[27–29]</sup> Therefore,  $^{29}\text{Si}$  NMR spectroscopy alone cannot exclude additional oxygen substitution leading to “mixed”  $\text{SiN}_n\text{O}_{4-n}$  environments. Nevertheless, we note that a relatively broad span of  $^{29}\text{Si}$  NMR chemical shifts has already been found from a still fairly small collection of nitridosilicates, ranging from  $\delta = -36$  ppm in  $\text{Y}_3\text{Si}_6\text{N}_{11}$  to  $\delta = -65$  ppm in  $\text{LaSi}_3\text{N}_5$ .<sup>[27–29]</sup> Thus the very strong shielding of the  $^{29}\text{Si}$  nuclei of the  $\text{SiN}_4$  tetrahedra may originate from a unique combination of structural factors (bond lengths and angles) in the present compound. From the single-crystal XRD analysis, we expect three distinct  $^{29}\text{Si}$  signals with relative intensities 1:4:4.

It is possible to reconcile the spectrum of Figure 6 with the proposed structure of  $\text{La}_{17}\text{Si}_9\text{Al}_4\text{N}_{33}$  by noting that if the  $^{29}\text{Si}$  signals from the two Si 16e sites overlap, a spectrum with two peaks of relative intensity 1:8 would result. This is not unlikely when considering that overlap between signals from *distinct*  $\text{SiN}_n\text{O}_{4-n}$  environments has previously been reported in the  $^{29}\text{Si}$  NMR spectra of oxynitridosilicates.<sup>[27,28,30]</sup> In fact, the width (FWHM  $\approx 10$  ppm) of the peak centred at  $\delta = 70$  ppm (Figure 6) is exceptional for a crystalline nitridosilicate. As neither of the two peaks from  $\text{La}_{17}\text{Si}_9\text{Al}_4\text{N}_{33}$  fitted well to a single Lorentzian, Gaussian or mixed lineshape, this indeed suggests that they either arise from several partially overlapping signals or that the peaks are broadened by residual MAS non-averaged dipolar couplings between  $^{29}\text{Si}$  and the quadrupolar spins in its surroundings ( $^{14}\text{N}$ ,  $^{27}\text{Al}$  and  $^{139}\text{La}$ ).<sup>[27,31]</sup> The ratio between the integrated peaks in Figure 6 was estimated to be  $1:(8.5 \pm 2)$ . The deviation from the ratio 1:8 may be due to different degrees of saturation of the three  $^{29}\text{Si}$  sites caused by differing  $T_1$  relaxation times or possibly from interfering signals of minor impurity phases.

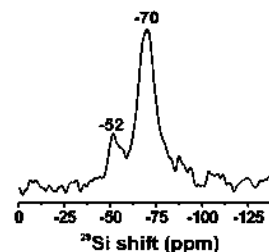


Figure 6.  $^{29}\text{Si}$  MAS spectrum recorded at 9.4 T employing MAS at 6.5 kHz. It is the result of 68 co-added signal transients using 30° excitation pulses and 50 min relaxation delays. 150 Hz FWHM Lorentzian broadening was applied in the data processing.

### Discussion

EDS microanalysis was performed on both the obtained crystals and the powder bulk samples and yielded 57(2)% La, 30(1)% Si, 13.3(9)% Al and 56(3)% La, 30(2)% Si, 13(1)% Al, which correspond to the formulae  $\text{La}_{17.0(6)}\text{Si}_{9.0(4)}\text{Al}_{4.0(3)}$  and  $\text{La}_{16.8(7)}\text{Si}_{9.1(5)}\text{Al}_{3.9(3)}$ , respectively. The analytical results are thus in very good agreement with the structural cation composition  $\text{La}_{17}\text{Si}_9\text{Al}_4$ , obtained by placing Al atoms on the 16e sites with  $x = 0.1800(3)$  and Si atoms on the remaining tetrahedral sites. Therefore, if all cation and anion positions are fully occupied, one can conclude by charge balancing that all anions are  $\text{N}^{3-}$  and that the compound formula is  $\text{La}_{17}\text{Si}_9\text{Al}_4\text{N}_{33}$ .

Considering the diffraction data alone, it cannot be ruled out, however, that the phase contains smaller amounts of oxygen. First, the starting materials  $\text{Si}_3\text{N}_4$  and  $\text{AlN}$  contain some oxygen, corresponding to an estimated O/N ratio in the final, fully nitrided mixture of about 0.5:33, which may partly explain why pure bulk samples were not obtained using stoichiometric metal compositions. Secondly, oxygen might also have been taken up by the sample during the

heat treatment, as we have observed for other syntheses, even though it was performed in a graphite furnace under a  $N_2$  gas flow. Furthermore, as described above, the amounts of the formed secondary phases could be significantly reduced by further carbothermal reduction and nitridation of the samples.

$^{27}\text{Al}$  NMR spectroscopy has provided direct evidence of O substitution at the N5 4c position by showing the presence of both  $\text{AlN}_3\text{O}$  and  $\text{AlN}_4$  tetrahedral units, whereas the  $^{29}\text{Si}$  NMR spectroscopic data could not rule out additional oxygen substitution. The smaller total anion charge resulting from O substitution is probably compensated by vacancies on some of the La sites, leading to a formula  $\text{La}_{17-x/3}\text{Si}_9\text{Al}_4\text{N}_{33-x}\text{O}_x$  ( $x \leq 1$ ). However, no reliable conclusions concerning La vacancies could be drawn from structure refinements. We see no way of incorporating more substantial amounts of oxygen without larger changes in the cation composition, which would contradict the results of the EDS analysis, the single crystal diffraction data, and the observed near constancy of the unit-cell parameter for bulk samples. We therefore conclude that the compound has a formula very close to  $\text{La}_{17}\text{Si}_9\text{Al}_4\text{N}_{33}$  but that it contains variable minor amounts of oxygen, with probable end-limit compositions being  $\text{La}_{17}\text{Si}_9\text{Al}_4\text{N}_{33}$  and  $\text{La}_{16.67}\text{Si}_9\text{Al}_4\text{N}_{32}\text{O}$ .

The unit-cell parameters and atomic coordinates of  $\text{La}_{17}\text{Si}_9\text{Al}_4\text{N}_{33}$  suggest that its structure could be a  $4 \times 4 \times 4$  superstructure of the perovskite type, similar to  $\text{Ce}_{16}\text{Si}_{15}\text{O}_6\text{N}_{32}$  for example,<sup>[6,9]</sup> which is notable as its structure contains silicon octahedrally coordinated by nitrogen. Following Liebau,<sup>[6]</sup> the latter formula may accordingly be rewritten as  $\text{Ce}_{16}(\text{Si}^{[6]}\text{Si}_{14}^{[4]}\square)(\text{O}_6\text{N}_{32}\square_{10})$ . The relationship to the cubic perovskite  $\text{ABX}_3$  structure rests on the fact that the atoms corresponding to A and B do not deviate significantly from the highly symmetrical positions in the ideal perovskite structure, even when the coordination number for B atoms is reduced from six to four. The anion X positions may, however, deviate extensively from their ideal positions and are expected to contain vacancies due to the decreased coordination number of the B atoms.

For  $\text{La}_{17}\text{Si}_9\text{Al}_4\text{N}_{33}$  the relationship with perovskite is not so close. While many of the La atoms are found in positions corresponding to perovskite A atoms, this set of positions is in addition occupied by SiI atoms (at the centres of the  $\text{Si}_5\text{N}_{16}$  zunyite-type clusters), N1 atoms (at the centres of the  $\text{Al}_4\text{Si}_4\text{N}_{17}$  clusters), and also contains vacancies [at the 4b sites (1/2, 1/2, 1/2)]. Further, the Al atom positions are significantly displaced from the positions corresponding to perovskite B atoms and the  $\text{Al}_4\text{Si}_4\text{N}_{17}$  clusters cannot readily be described as part of a perovskite structure. It should also be noted that the  $\text{Al}_4\text{Si}_4\text{N}_{17}$  clusters cannot be described as being a part of an anion close packing.

According to the formula  $\text{La}_{17}\text{Si}_9\text{Al}_4\text{N}_{33}$ , the compound is one of the rare examples of a pure nitridoaluminosilicate. More noteworthy, however, is that  $\text{La}_{17}\text{Si}_9\text{Al}_4\text{N}_{33}$  is a nitrido(alumino)silicate with a structure where all the tetrahedral atoms are part of isolated complex anions or clusters that contain only, or predominantly, N atoms. Nitridosilicate crystal chemistry differs from that of oxosilicates mainly

due to the common occurrence of  $\text{N}^{(3)}$ , and to a much less extent of  $\text{N}^{(4)}$ , atoms.<sup>[9]</sup> For oxonitridosilicates and sialons, the crystal chemistry is more similar to that of oxosilicates, especially for low N/O ratios. As the T/X ratio increases [ $T = (\text{Si}/\text{Al})$  and  $X = (\text{N}/\text{O})$ ] the structures exhibit a condensation of the tetrahedra in the sequence of isolated  $\text{TX}_4$  tetrahedra  $\rightarrow$  isolated  $\text{T}_2\text{X}_7$  groups  $\rightarrow$  rings or chains of tetrahedra  $\rightarrow$  layers of tetrahedra  $\rightarrow$  frameworks of tetrahedra.<sup>[11]</sup> Structures containing more complex isolated clusters built up from  $\text{TX}_4$  tetrahedra are virtually non-existent for all of these types of silicates. The compound  $\text{La}_{17}\text{Si}_9\text{Al}_4\text{N}_{33}$  has a T/X ratio of 1:2.54, from which one might anticipate a structure containing rings, chains or sheets of tetrahedra. Instead, the structure contains isolated tetrahedral clusters and 48.5%  $\text{N}^{(1)}$ , 48.5%  $\text{N}^{(2)}$  and 3.0%  $\text{N}^{(4)}$  atoms. Despite its high nitrogen and silicon content, there are no  $\text{N}^{(3)}$  atoms, which are the common structural characteristic for nitridosilicates.

## Experimental Section

Powder samples of  $\text{La}_{17}\text{Si}_9\text{Al}_4\text{N}_{33}$  were prepared at 1500–1650 °C in a graphite furnace under nitrogen, from La metal (Chempure, 99.9%),  $\text{Si}_3\text{N}_4$  (UBE, SN-E10) and AlN (H. C. Starck, Berlin, grade A) as starting materials. During the synthesis the La metal reacts with  $\text{N}_2$  to form reactive LaNd. The powders were mixed, in amounts of ca. 1 g, and ground in a dry-box under argon to prevent oxidation of the La metal, and then placed in Nb tubes that were sealed with parafilm during the transfer to the furnace. In a typical run, the sample was heated to the synthesis temperature over 2 h, kept there for 12 h, then cooled to 1200 °C over 4 h, whereupon the furnace was switched off. Yellow to orange single crystals were found in preparations at 1650 °C.

The heat-treated powder samples were characterised by their X-ray powder patterns, which were recorded with a Guinier–Hägg camera, using  $\text{Cu-K}_{\alpha 1}$  radiation and Si as internal standard. The data were evaluated using a film scanner system<sup>[32]</sup> and, for the majority of patterns, the Rietveld program FullProf.<sup>[33]</sup> Energy-dispersive X-ray (EDX) microanalyses of the metal composition were made using a JEOL 820 scanning electron microscope equipped with a LINK AN10000 EDX system. Electron diffraction (ED) studies were carried out with a JEOL 200FX transmission electron microscope (TEM), operating at 200 kV, in order to confirm the crystal system and space group. Single-crystal X-ray diffraction (XRD) data for  $\text{La}_{17}\text{Si}_9\text{Al}_4\text{N}_{33}$  were collected with a STOE image-plate detector system (IPDS), using a Siemens rotating anode and  $\text{Mo-K}_{\alpha}$  radiation, up to  $2\theta = 52^\circ$  and  $d$ -values  $\geq 0.81 \text{ \AA}$  (Table 4). The STOE IPDS software package<sup>[34]</sup> was used for indexing and integration.

Further details of the crystal-structure investigations may be obtained from the Fachinformationzentrum, 76344 Eggenstein-Leopoldshafen, Germany, on quoting the depository number CSD-416358.

Magic-angle spinning (MAS) NMR experiments were carried out on a finely ground powder of  $\text{La}_{17}\text{Si}_9\text{Al}_4\text{N}_{33}$  using a Varian/Chemagnetics Infinity-400 spectrometer at a magnetic field of 9.4 T, with the Larmor frequencies 79.50 and  $-104.28 \text{ MHz}$  for  $^{29}\text{Si}$  and  $^{27}\text{Al}$ , respectively. 6-mm and 4-mm probeheads were employed for  $^{29}\text{Si}$  and  $^{27}\text{Al}$  acquisitions, respectively. Chemical shifts are reported in

Table 4. Refinement data for  $\text{La}_{17}\text{Si}_9\text{Al}_4\text{N}_{33}$ .

|  |  |
|--|--|
| Crystal form   | cube   |
| Crystal size [mm]  | $0.02 \times 0.02 \times 0.02$   |
| Radiation [Å]  | Mo- $K_\alpha$ (0.71073 Å)   |
| $\mu$ (mm <sup>-1</sup> )  | 19.80  |
| Absorption correction  | numerical from shape   |
| Range of $h, k, l$   | $-10 \rightarrow h \rightarrow 10$<br>$0 \rightarrow k \rightarrow 13$<br>$1 \rightarrow l \rightarrow 18$ |
| No. of measured reflections  | 6463   |
| No. of independent reflections   | 410  |
| No. of observed reflections  | 294  |
| Criterion for observed reflections   | $I > 3\sigma(I)$   |
| $R_{\text{int}}$   | 0.063  |
| $2\theta$ max. [°]   | 52.0   |
| Refinement on  | $F$  |
| No. of reflections used in the refinement  | 294  |
| No. of parameters used   | 34   |
| $R [I > 3\sigma(I)]$   | 0.019  |
| $wR [I > 3\sigma(I)]$  | 0.019  |
| $R$ (all)  | 0.031  |
| $wR$ (all)   | 0.023  |
| $S$  | 1.15   |
| $\Delta\rho_{\text{max}}, \Delta\rho_{\text{min}}$ (e <sup>-</sup> Å <sup>-3</sup> ) | +1.5, -1.0   |

deshielding ( $\delta$ ) units of ppm, referenced with respect to TMS ( $^{29}\text{Si}$ ) and  $\text{Al}^{3+}(\text{aq})$  ( $^{27}\text{Al}$ ). Additional experimental parameters are given in the figure captions.

## Acknowledgments

We thank Z. Weng for instrumental NMR support, A. Sohler and L. Del Villano for their help during the syntheses and NMR characterisations, respectively, Dr. J. Garcia-Garcia for the EDS analyses, and Prof. W. Schnick for valuable discussions. S.E. holds a research fellowship from the Royal Academy of Sciences financed by the Knut and Alice Wallenberg Foundation. This work was supported by the Swedish Research Council (VR) and by the Carl Tryggers Foundation.

- [1] T. Ekström, M. Nygren, *J. Am. Ceram. Soc.* **1992**, 75, 259.
- [2] W. Schnick, H. Huppertz, *Chem. Eur. J.* **1997**, 3, 679.
- [3] W. Schnick, H. Huppertz, R. Lauterbach, *J. Mater. Chem.* **1999**, 9, 289.
- [4] H. Huppertz, W. Schnick, *Chem. Eur. J.* **1997**, 3, 249.
- [5] H. Yamane, F. J. DiSalvo, *J. Alloys Compd.* **1996**, 240, 33.
- [6] K. Köllisch, W. Schnick, *Angew. Chem. Int. Ed.* **1999**, 38, 357.

- [7] F. Liebau, *Structural Chemistry of Silicates*, Springer-Verlag, Berlin, **1985**.
- [8] H. Huppertz, W. Schnick, *Angew. Chem. Int. Ed.* **1996**, 35, 1983.
- [9] F. Liebau, *Angew. Chem. Int. Ed.* **1999**, 38, 1733.
- [10] K. Köllisch, PhD Thesis, University of Bayreuth, Germany, **2001**.
- [11] D. P. Thompson, *Mater. Sci. Forum* **1989**, 47, 21.
- [12] F. Ottinger, PhD Thesis, Eidgenössische Technische Hochschule, Zürich, Diss. ETH Nr. 15624, **2004**.
- [13] J. Grins, S. Esmailzadeh, Z. Shen, *J. Am. Ceram. Soc.* **2003**, 86, 727.
- [14] J. P. Morniroli, J. W. Steeds, *Ultramicroscopy* **1992**, 45, 219.
- [15] A. Altomare, M. C. Burla, M. Camalli, G. L. Cascarano, C. Giacovazzo, A. Guagliardi, A. G. G. Moliterni, G. Polidori, R. Spagna, *J. Appl. Crystallogr.* **1999**, 32, 115.
- [16] D. J. Watkin, C. K. Prout, J. R. Carruthers, P. W. Betteridge, *CRYSTALS Issue 11*, Chemical Crystallography Laboratory, Oxford, UK, **1999**.
- [17] J. Lima-De-Faria, E. Hellner, F. Liebau, E. Makovicky, E. Parthé, *Acta Crystallogr. Sect. A* **1990**, 46, 1.
- [18] W. B. Kamb, *Acta Crystallogr.* **1960**, 13, 15.
- [19] J. Fernández-Urban, S. Esmailzadeh, manuscript to be published.
- [20] M. Woike, W. Jeitschko, *J. Solid State Chem.* **1997**, 129, 312.
- [21] K. Köllisch, H. A. Höpfe, H. Huppertz, M. Orth, W. Schnick, *Z. Anorg. Allg. Chem.* **2001**, 627, 1371.
- [22] A. Medek, J. S. Harwood, L. Frydman, *J. Am. Chem. Soc.* **1995**, 117, 1279.
- [23] D. Massiot, B. Touzo, D. Trumeau, J. P. Coutures, J. Virlet, P. Florian, P. J. Grandinetti, *Solid State NMR* **1996**, 6, 73.
- [24] M. E. Smith, *J. Phys. Chem.* **1992**, 96, 1444.
- [25] R. Dupree, M. H. Lewis, M. E. Smith, *J. Appl. Crystallogr.* **1988**, 21, 109.
- [26] E. Lippmaa, A. Samoson, M. Mägi, *J. Am. Chem. Soc.* **1986**, 108, 1730.
- [27] R. Dupree, M. H. Lewis, M. E. Smith, *J. Am. Chem. Soc.* **1989**, 111, 5125.
- [28] R. K. Harris, M. J. Leach, D. P. Thompson, *Chem. Mater.* **1989**, 1, 336.
- [29] T. C. Ekström, K. J. D. MacKenzie, M. J. Ryan, I. W. M. Brown, G. V. White, *J. Mater. Chem.* **1997**, 7, 505.
- [30] A. Koroglu, D. P. Thompson, D. C. Apperley, R. K. Harris, *J. Solid State Chem.* **2004**, 177, 2530.
- [31] R. K. Harris, A. A. Olivieri, *Prog. Nucl. Magn. Reson. Spectrosc.* **1992**, 24, 435.
- [32] K. E. Johansson, T. Palm, P.-E. Werner, *J. Phys. E* **1980**, 13, 1289.
- [33] J. Rodriguez-Carjaval, *FullProf98* and *WinPLOTR*: New Windows 95/NT Applications for Diffraction Commission for Powder Diffraction, International Union for Crystallography, Newsletter no. 20 (May–August), summer **1998**.
- [34] *STOE IPDS software manual*, version 2.87, December **1997**.

Received: March 28, 2006

Published Online: August 3, 2006